*Avrupa Bilim ve Teknoloji Dergisi*
*Özel Sayı 37, S. 147-155, Haziran 2022*

***Araştırma Makalesi***

www.ejosat.com ISSN:2148-2683

*European Journal of Science and Technology*
*Special Issue 37, pp. 147-155, June 2022*

***Research Article***

# Fusion of Multi-Focus Images using Jellyfish Search Optimizer

Fatma Çıtıl[1*], Rifat Kurban[2], Ali Durmuş[3], Ercan Karaköse[4]

[1*] Kayseri Üniversitesi, Lisansüstü Eğitim Enstitüsü, Elektrik-Elektronik Mühendisliği, Kayseri, Türkiye (ORCID: 0000-0001-9794-4996), citil.fatmaa@gmail.com
[2] Kayseri Üniversitesi, Teknik Bilimler Meslek Yüksekokulu, Bilgisayar Teknolojileri Bölümü, Kayseri, Türkiye (ORCID:0000-0002-02772210),rifatkurban@gmail.com
[3] Kayseri Üniversitesi, Teknik Bilimler Meslek Yüksekokulu, Elektrik ve Enerji Bölümü, Kayseri, Türkiye (ORCID: 0000-0001-8283-8496), alidurmus@kayseri.edu.tr
[4] Kayseri Üniversitesi, Mühendislik Mim. ve Tasarım Fakültesi, Temel Bilimler Bölümü, Kayseri, Türkiye (ORCID: 0000-0001-5586-3258), ekarakose@kayseri.edu.tr

(5th International Symposium on Innovative Approaches in Smart Technologies– 28-29 May 2022)

(**DOI:** 10.31590/ejosat.1136956)

**ATIF/REFERENCE:** Citil, F., Kurban, R., Durmus, A. & Karaköse, E. (2022). Fusion of Multi-Focus Image using Jellyfish Search Optimizer. *European Journal of Science and Technology*, (37), 147-155.

**Abstract**

When obtaining an image of a scene, the lens focuses on objects at a certain distance, and objects at other distances are blurred. This is called the limited depth of field problem. An approach for solving this problem is multi-focus image fusion. A clearer view of the entire scene is obtained by using the multi-focus image fusion method. For this method, at least two images captured at different focuses are combined. Various algorithms have been developed for multi-focus image fusion methods. For multi-focus image fusion, pixel-level block-based methods are commonly used. The block size is a factor that significantly affects the fusion performance. As a result, the block size parameter must be improved. The Jellyfish search optimization algorithm (JSA) is used to propose a block-based multi-focus image fusion approach based on the optimal selection of clearer image blocks from source images. The results of DWTPCA, DCHWT, APCA, PCA, SWTDWT and SWT methods, which are traditional image fusion methods, and ABC (artificial bee colony) and JSA optimization algorithms, which are metaheuristic methods, are compared. In addition, it has been determined that the JSA method has better performance than other traditional methods when compared both visually and quantitatively.

**Keywords:** Image Fusion, Extending Depth of Field, Jellyfish Search Optimization Algorithm.

# Denizanası Arama Optimizasyon Algoritması ile Çok-Odaklı Görüntülerin Birleştirilmesi

**Öz**

Bir sahnenin görüntüsü çekilirken lens belirli bir mesafede bulunan nesnelere odaklanır ve diğer uzaklıkta bulunan nesneler ise bulanık olur. Buna sınırlı alan derinliği problem adı verilir. Çok-odaklı görüntü birleştirme yöntemi bu problemi çözmek için kullanılan bir yöntemdir. Çok-odaklı görüntü birleştirme yöntemi kullanılarak sahnenin tamamının net görüntüsü elde edilir. Bu yöntem için farklı odaklarda çekilmiş en az iki görüntü birleştirilir. Çok-odaklı görüntü birleştirme için klasik görüntü birleştirme yöntemlerine ek olarak çeşitli algoritmalar geliştirilmiştir. Çok-odaklı görüntü birleştirme için piksel düzeyinde blok tabanlı yöntemler yaygın olarak kullanılır. Kullanılabilecek blok boyutu birleştirme performansını önemli ölçüde etkileyen bir faktördür. Dolayısıyla blok boyutunun optimize edilmesi gerekmektedir. Bu makalede, deniz anası arama (JSA) optimizasyon algoritması kullanılarak kaynak görüntülerden daha net görüntü bloklarının optimal seçimine dayanan, blok tabanlı çok-odaklı görüntü birleştirme yöntemi önerilmiştir. Geleneksel görüntü birleştirme yöntemlerinden olan DWTPCA, DCHWT, APCA, PCA, SWTDWT ve SWT metotları ile metasezgisel yöntemlerden olan yapay arı kolonisi (ABC) ve JSA sonuçları kıyaslanmıştır. Ayrıca JSA metodunun hem görsel hem de nicel olarak karşılaştırıldığında diğer yöntemlerden daha iyi performansa sahip olduğunu belirlenmiştir.

**Anahtar Kelimeler:** Görüntü Birleştirme, Sınırlı Alan Derinliği Artırma, Deniz Anası Arama Optimizasyon Algoritması.

[*] Corresponding Author: Kayseri Üniversitesi, Mühendislik Fakültesi, Elektrik Elektronik Mühendisliği Bölümü, Kayseri, Türkiye, ORCID: 0000-0001-9794-4996, citil.fatmaa@gmail.com

# 1. Introduction

Due to the fact that optical lenses have a limited depth of field, it is difficult to achieve a sharp and fully focused image with all objects in focus. A series of images with different focus settings are combined using image fusion techniques. This is how the limited depth of field problem is solved. The fusion of source images obtained at two or more distinct focuses to form a single completely focused image is known as multifocus image fusion. Image fusion is used to create a fusion image that is higher in quality and contains more information than the original photos. Blur is a factor that significantly reduces information in an image. Multifocus image fusion methods allow us to obtain a fused image with more details than the input images (Goshtasby & Nikolov, 2007). Various fusion methods enhance the restricted depth of field of lenses. Multifocus image creation methods are used in image processing, remote sensing, medical imaging object recognition, computer vision and other applications. There are several different techniques that can be used to carry out multifocus fusion. Multi-focus image fusion methods can be examined in four main groups; hybrid methods, spatial domain and transformation domain methods, and deep learning-based methods which on very popular in recent years (Garg, Gupta, & Kaur, 2014; Irshad, Kamran, Siddiqui, & Hussain, 2009; Meher, Agrawal, Panda, & Abraham, 2019). Spatial domain methods are aggregation methods that deal directly with pixels and operations based on pixel density (Nejati et al., 2017; Nejati, Samavi, & Shirani, 2015). Fusion is performed without any transformation on the density of pixels in the source image, whereas transform field methods use wavelet transform or pyramid decompositions to exploit information at different scales or multiple resolutions thereby transforming the source images, then reconstructing the fused image. Pixel-based, block-based, and region-based methods are the three types of spatial domain approaches. (Zhang et al., 2020). In these methods, the aim is to select pixels, blocks or regions that contain more information. In pixel-based methods, sharpness analysis is performed for each pixel in the image separately and a fusion image is created by selecting the pixels that are understood to be clear. The input images are split into tile-like chunks of defined size in block-based approaches. Each block's activity level is measured using this way. In the literature, many approaches for the spatial and transformation domains have been offered. Aslantas and Toprak presented a pixel-based multi-focus image domain approach based on the basic premise that focussed and unfocused pixels of source images may be recognized by estimating the point spread functions (PSF) of these images. (Veysel Aslantas & Toprak, 2014). The original pixel values of the source images are not maintained in the fused image when using transform domain techniques. Furthermore, the implementation of these approaches is difficult, and algorithm implementation takes time. The pixel-based image fusion approach is straightforward and well-suited to real-time image processing. However, it ignores the relationship between surrounding pixels, and this can cause undesirable side effects such as increased or decreased contrast in the fused image. To increase the quality of the combined image, many block-based multifocus image fusion approaches have been developed. These approaches work by picking sharper image chunks among the original photos to generate a fused image. However, the fixed block size may not apply to every application (Banharnsakun, 2019). Another undesirable block size is one that is either too little or too huge. To get a combined image incorporating the sharper regions of the source photos, block size optimization is required. Algorithms have proved to handle optimization issues in many sectors of science and engineering in recent years, according to research. Zhang et al. developed the concept of image blocks and evolutionary search algorithms for multifocus image fusion at the pixel level (Bai, Liu, Chen, Wang, & Zhang, 2016). An adaptive genetic search method selects the optimum image using a different mix of image blocks (GA). However, the GA algorithm's processing speed is insufficient. Aslantaş and Kurban provide an ideal approach for multifocus image fusion in the spatial domain based on the differential evolution (DE) algorithm in order to optimize the block size in order to maximize the sharpness of the fused image (Veysel Aslantas & Kurban, 2010). Agrawal et al. Offer a pixel-based multifocus image fusion japproach based on independent component analysis (ICA) and the bacterial search optimization (BFO) algorithm. (Agrawal, Swain, & Dora, 2013).

The Jellyfish search algorithm (Chou and Truong, 2021), which is one of the innovative metaheuristic algorithms that has come to the fore with numerous advantages, is used to present an efficient and resilient multifocus image fusion approach based on the selection of sharper image blocks from source images. Source images are split up into blocks for the first stage. The block size is then chosen using JSA strategies. In the next step, the spatial image frequency is used to compare the blocks with sharper images with their counterparts in the source images, and the variance metric is used to measure the overall quality of the combined image. In addition, we implemented several new methods for comparison with our proposed work, including ABC, algorithms for optimization of block size alongside traditional fusion methods. The accomplishment of developing an effective and robust approach for multi-focus image fusion with quicker convergence utilizing newly developed JSA to optimize the block size to enhance the sharpness of the fused image is the key contribution of this study. The remainder of the article is organized as follows. A brief introduction to block-based multi-focus image fusion and focus measurements is described in Section 2. Adopting the best ever JSA in multi-focus image fusion is proposed in Section 3. In section 4, experimental results are presented. It is discussed in section 5. The article ends in chapter 6.

# 2. Methods for Image Fusion and Quality Metrics

## 2.1. Image Fusion Methods

R.Amutha proposed a technique for multi-focus image fusion based on the Discrete Cosine Transform (DCT) (Phamila & Amutha, 2014). The source photos are separated into blocks using this manner. Each block's DCT coefficients are determined. For image fusion, the modified block with the highest AC coefficient is chosen. On fused DCT blocks, consistency checking is

conducted. To reconstitute the original fused image, inverted DCT is applied to the fused DCT coefficients. (Cao et al., 2014). The input images are deconstructed using db3 wavelets and a discrete wavelet transform with one or two stages of decomposition in the image fusion approach, which employs the discrete wavelet transform based on the mean of the main components. The input images' detailed and approximate coefficients are subjected to principal component analysis. For multiscale coefficients, principal components are evaluated. The input images' detailed and approximate coefficients are subjected to principal component analysis. For multiscale coefficients, principal components are evaluated.The fusion is calculated across each column (Vijayarajan, Muttan, & Communications, 2015). Wavelets, which are fundamentally linear transformations, are used in the Discrete Wavelet Transform (DWT). The wavelet transform image fusion method examines two DWT coefficients in the input images and picks the one with the highest value. The Stationary wavelet transform (SWT) method involves the following steps: obtaining the focused areas in the source images. The focused image is reconstructed using an inverse stationary wavelet transformThe fusion outcome is influenced by the wavelet basis and coefficient selection techniques. It is resistant to rotation and translation (Wang et al., 2005). DWTPCA and SWTDCT methods are hybrid methods that use the advantages of spatial domain and transformation field methods and combine them in one method.

## 2.2.Focus Quality Metrics for Image Fusion

The spatial frequency (SF) is an image quality indicator that indicates how active a image is overall (Eskicioglu & Fisher, 1995). The spatial frequency is defined as:

$$SF = \sqrt{RF^2 + CF^2} \quad (1)$$

where *RF* is the row frequency and *CF* is the column frequency (Eskicioglu & Fisher, 1995; Shutao Li, Kwok, & Wang, 2001).

$Q_p^{AB/F}$ is used to evaluate the performance of fusion systems at the pixel level and has three components. The first is a traditional multi-resolution fusion system that employs a subband pixel selection approach for pyramid fusion. The second is the Quad Mirror Filter decomposition approach using a cross-band selection technique for pyramid fusion, and the third is a background/foreground-based computationally efficient system separation and fusion process. (Xydeas & Petrovic, 2000).

SCD (Sum of Correlations of Differences) is a statistic for image fusion image quality. It's based on the relationship between the source images and the difference images calculated using the merged image. Rather than measuring merged image quality directly using correlations between source and merged images, the suggested metric determines quality by taking into account the source images and their impact on the combined image. (V Aslantas, Bendes, & communications, 2015).

The QY metric was defined by Yang (Shanshan Li, Hong, & Wu, 2008) which works on structure similarity for converged image quality assessment.

# 3. JellyFish Search Algorithm (JSA)

The artificial Jellyfish Search (JSA) algorithm is a metaheuristic algorithm. This algorithm was developed by Chou and Turong in 2021 inspired by Jellyfish's movements in oceans to solve complex numerical optimization problems (Chou and Truong, 2021). Jellyfish foraging behavior includes mobility (both passive and active) within a swarm, a transitory control mechanism for switching between different motions, and convergence with jellyfish blooms. Jellyfish can be found at various temperatures and depths. They are bell-shaped, some less than one centimeter in diameter and others several centimeters. They are available in a variety of sizes, colors, and forms. Many animals have adapted to the maritime environment in unique ways. Jellyfishes utilize their arms to move nutrition into their mouths. Some of them take what the current gives them. Other jellyfish actively chase their food and use their tentacles to immobilize them (Bastian et al., 2014; Dorigo, Birattari, & Stutzle, 2006). The characteristics of jellyfish allows controlling the motions. Their umbrella shaped undersides allows water to escape and propelling them forward. Despite having such an capability, they generally slide in water due to the tides and currents (Fossette, Putman, Lohmann, Marsh, & Hays, 2012). In favorable conditions, jellyfish can form swarms. Jellyfish flower is a very large jellyfish mass. Jellyfish are slow swimmers. Therefore, adjusting them to the current is very important to protect the flowers and prevent them from getting stuck. Factors affecting herd formation are ocean currents, available nutrients, temperature and oxygen availability. The most critical of these elements is ocean currents, as they can create swarms of jellyfish (Brotz, Cheung, Kleisner, Pakhomov, & Pauly, 2012; Dong, Liu, & Keesing, 2010; Fossette et al., 2015). The capacity to spawn practically anywhere in the water is due to each jellyfish's individual motions within the swarm and its ability to follow the ocean current to form jellyfish blooms. The amount of food varies where jellyfish go; thus, the best place will be determined when the amount of food is compared.

Three rules govern the JSA optimization algorithm:

1. A "time control system" handles the transition between both forms of movement. Jellyfish follow the ocean current or migrate into the swarm.

2. In pursuit of food, jellyfish travel across the ocean. Where there is a greater abundance of food, they are more attracted.

3. The location and related goal function determine the amount of food found.

## 3.1. Ocean Current

There are a lot of nutrients in the ocean current. Jellyfish tend to go to large amounts of food. So, they go towards the ocean current. All trends (*t*) influence the path of the current, from every jellyfish in the water to the one in the best position right now:

$$\vec{t} = \frac{1}{n_{pop}} \sum \vec{t_i}, = \frac{1}{n_{pop}} \sum (X^* - e_c X_i) \; = X^* - e_c \frac{\sum X_i}{n_{pop}} = X^* - e_c \mu \quad (2)$$

$$df = e_c \mu \quad (3)$$

$\vec{t}$ determined as;

$$\vec{t} = X^* - df \quad (4)$$

The distance ± βσ around the jellyfish average position contain the specific probability of all remaining jellyfishes, where σ is the std. dev.

$$df = \beta \times \sigma \times rand^{f}\ (0,\ 1) \quad (5)$$

$$\sigma = rand^{a}\ (0,\ 1) \times \mu \quad (6)$$

From here;

$$df = \beta \times rand^{f}\ (0,\ 1) \times rand^{a}\ (0,\ 1) \times \mu \quad (7)$$

$$df = \beta \times rand(0,\ 1) \times \mu \quad (8)$$

$$e_c = \beta \times rand(0,\ 1) \quad (9)$$

$$\vec{t} = X^{*} - \beta \times rand(0,\ 1) \times \mu \quad (10)$$

The new position of each jellyfish is given as follows:

$$X_i(t+1) = X_i(t) + rand(0,\ 1) \times \vec{t} \quad (11)$$

$$X_i(t+1) = X_i(t) + rand(0,\ 1) \times (X^{*} - \beta \times rand(0,\ 1) \times \mu) \quad (12)$$

where $n_{pop}$ :is population size of jelly fish. *X**, currently the best-positioned jellyfish in the herd, $e_c$ attractiveness coefficient and $\mu$ is average position of the jellyfishes, *df* represents the measure of gap among the best available position of a jellyfish and the average position of remanining jellyfishes.

### 3.2. Jellyfish Swarm

Jellyfish move in flocks in two ways, active (type B) and passive (type A) (Mariottini & Pane, 2010; Zavodnik, 1987). Most jellyfish demonstrate type A movement while the swarm is first formed. They display greater and more type B motions with time. Type A motion describes the movement of jellyfish around their present place and is determined by each jellyfish's current position.

$$X_i(t+1) = X_i(t) + \gamma \times rand(0,1) \times (U_b - L_b) \quad (13)$$

where, respectively, $U_b$ and $L_b$, represent the upper bound and lower bound of the search spaces; $\gamma > 0$ is a coefficient of motion related to the length of motion around the jellyfish's positions.

A different jellyfish (j) from the one of interest is randomly selected to mimic B-type motion. The direction (*dir*) of motion is determined by using a vector of $i^{th}$ jellyfish to the chosen $j^{th}$ jellyfish. The jellyfish move towards the first when the amount of food in position (j) of the selected jellyfish exceeds the amount in position (i) of the jellyfish of interest. If the amount of food available to the chosen jellyfish (j) is less than that available to the matching jellyfish (i) it will migrate away from it immediately. Thus, each jellyfish moves in the better direction to find the food in the flock.

$$\overrightarrow{step} = X_i(t+1) - X_i(t) \quad (14)$$

$$\overrightarrow{step} = rand(0,1) \times \overrightarrow{dir} \quad (15)$$

$$\overrightarrow{dir} = \begin{cases} X_j(t) - X_i(t), & f(X_i) \geq f(X_j) \\ X_j(t) - X_i(t), & f(X_i) < f(X_j) \end{cases} \quad (16)$$

$$X_i(t+1) = -X_i(t) + \overrightarrow{step} \quad (17)$$

### 3.3. Time Control Mechanism

Jellyfish are drawn to the ocean current because of the abundance of nutrient-rich food it carries (Dorigo, M., Birattari, M., & Stutzle, T. ,2006). Swarms occur as more jellyfishes congregate over time. Wind or temperature variations of the currents causes the some of the jellyfishes to travel towards another current and form a new swarm. In a jellyfish swarm, the jellyfish travel through two types of motions: type A (passive movements) and type B (active movements). Initially, type A is favoured; nevertheless, as time passes, type B is preferred. To imitate this condition, a time control method is used. The time control mechanism that governs the movement between jellyfish moving in the swarm and following the ocean current includes the c(t) function and the $C_o$ constant. The random value of the time control function varies over time from 0 to 1.

$$c(t) = \left| \left(1 - \frac{1}{Max_{iter}}\right) \times (2 \times rand(0,1) - 1) \right| \quad (18)$$

The time control function is defined by the equation. The jellyfish follows the ocean current when its value surpasses $C_o$. They move in the swarm when its value is less than $C_o$. An exact value of $C_o$ is obscure and controlling the time varies randomly from 0 to 1. t is the time defined as the number of iterations, and The maximum number of repetitions with a parameter initialized is known as "max iterations". Exploration and exploitation are the two major stages of a meta-heuristic algorithm. (Xu & Zhang, 2014). Exploration is movement towards an ocean current. Exploitation is the movement of the jellyfish within the swarm. The time control ability switches between exploration and exploitation. The likelihood of discovery initially outweighs the possibility of utilizing it to locate regions with ideal placements. However, the exploitation probability rate outweighs the rate of exploration, and the swarm finds the best position within the allocated zones.

## 4. Experimental Results

In this study, a new method with better performance than the studies in the literature, is proposed by comparing different methods for multi-focus image fusion. DWTPCA, DCHWT, APCA, PCA, SWTDWT and SWT methods are evaluated using quality metrics such as Qp_ABF, QSCD, Qy, QSF and Qstd on two multi-focus image pairs taken from Lytro dataset and another two multi-focus image pairs taken with Nikon D3500 digital camera. Experiments are carried out on a laptop computer with 2.8 GHz Intel Core processor and 16GB RAM with Matlab programming language. The schematic diagram of the proposed JSA based image fusion method is given in Figure 1.

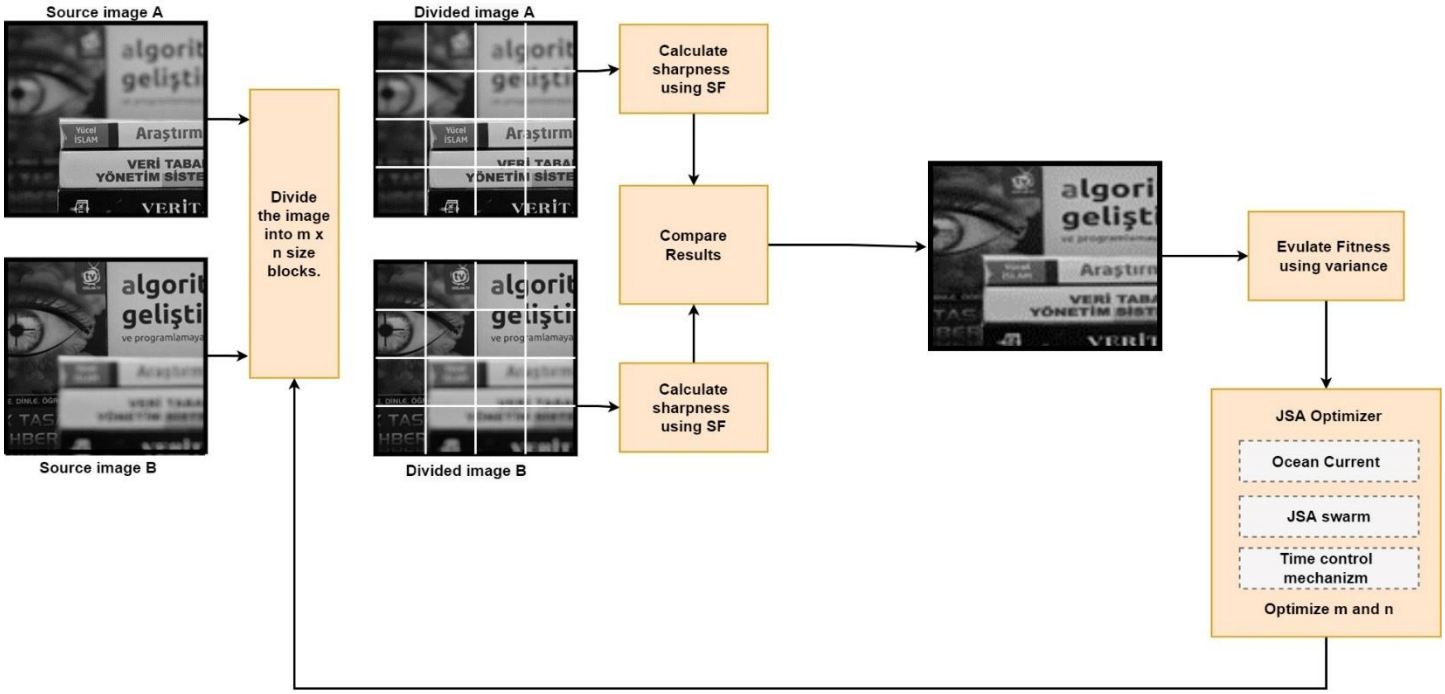


***Figure 1***. *The schematic diagram of the JSA based image fusion method*

## 4.1. Numerical Results

In Figure 2, four different source images are given. Figure 2 (a), (b), (c) and (d) are taken with the Nikon D3500 digital camera. Figure 2 (g), (h), (e) and (f) are obtained from the Lytro dataset (Liu, Wang, Cheng, Li, & Chen, 2020). In the analysis of the results, the best method on the basis of each metric is shown in red, the second-best method in blue, and the third-best method in green.

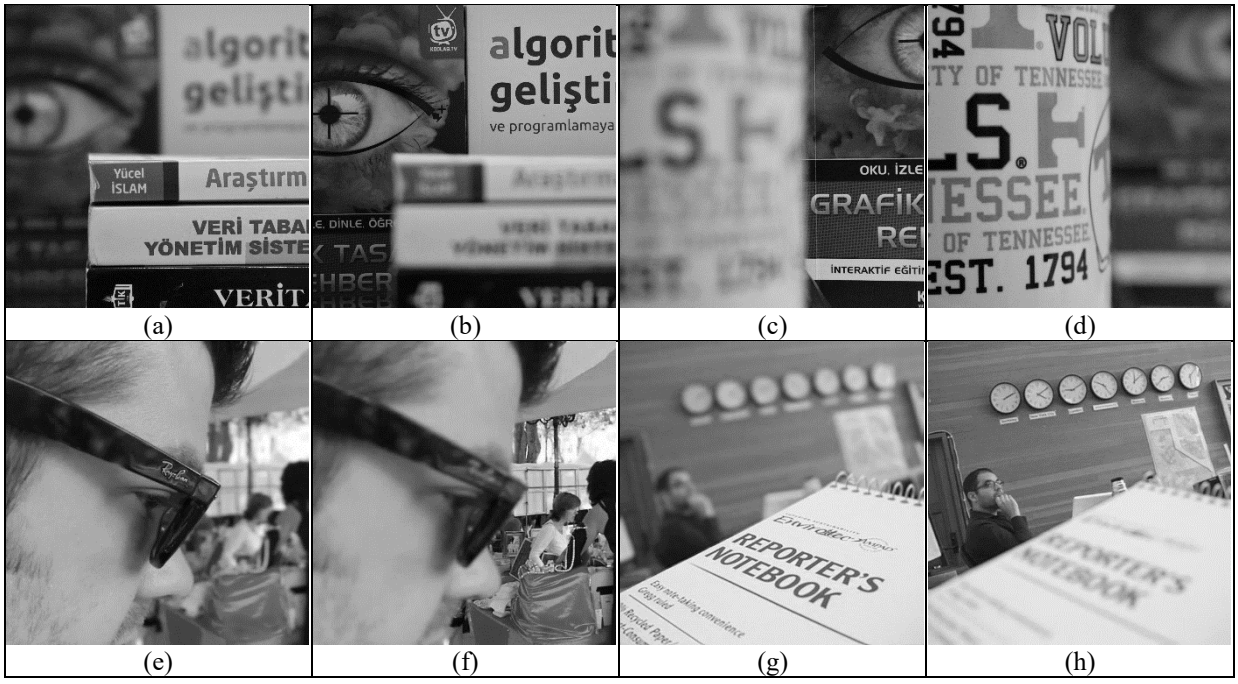


***Figure 2***: *Source images used in the study*

***Table 1:*** *Numerical results of the quality metrics of compared fusion methods by using source images (a) and (b) in Figure 2.*

| Fused image 1 | Qp_ABF | QSCD | Qy | QSF | Qstd | CPU Time |
|---|---|---|---|---|---|---|
| **DWTPCA** | 0,5412 | 0,4693 | 0,9153 | 16,9985 | 60,3942 | 0,0373 |
| **DCHWT** | 0,6785 | 0,6621 | 0,9629 | 28,2454 | 64,0712 | 0,6145 |
| **APCA** | 0,5537 | 0,4734 | 0,9105 | 16,7488 | 60,3407 | 0,0872 |
| **PCA** | 0,5465 | 0,4673 | 0,9061 | 16,6308 | 60,2780 | 0,0037 |
| **SWTDCT** | 0,4812 | 0,4011 | 0,8768 | 28,6786 | 62,5037 | 1,0134 |
| **SWT** | 0,6345 | 0,5469 | 0,9387 | 24,0612 | 61,4136 | 0,0574 |
| **ABC** | 0,7412 | 0,7086 | 0,9817 | 29,9223 | 65,6519 | 2,3084 |
| **JSA** | 0,7414 | 0,7087 | 0,9817 | 29,9257 | 65,6532 | 1,2568 |

Quantitative fusion results of Figure 2 (a) and (b) source images using DWTPCA, DCHWT, APCA, PCA, SWTDWT and SWT, ABC and JSA methods are given in Table 1. According to Table 1, JSA is better than other methods in terms of all quality metrics. The second-best result is the ABC method for all metrics, and the third best result is DCHWT in terms of Qp_ABF, QSCD and Qstd metrics. When the CPU time consumption of the methods are compared, PCA method gets the fastest results from the traditional methods, the DWTPCA method is the second and the SWT method is the third. In addition, it is seen that the JSA method, which is one of the metaheuristic methods, can converge to the optimal solution faster than the ABC method.

**Table 2:** *Numerical results of the quality metrics of compared fusion methods by using source images (c) and (d) in Figure 2.*

| Fused image 2 | Qp_ABF | QSCD | Qy | QSF | Qstd | CPU Time |
|---|---|---|---|---|---|---|
| **DWTPCA** | 0,4132 | 0,5950 | 0,9484 | 16,5128 | 54,8139 | 0,0087 |
| **DCHWT** | 0,7082 | 0,8622 | 0,9708 | 24,4752 | 58,8326 | 0,6058 |
| **APCA** | 0,4823 | 0,6154 | 0,9038 | 14,9379 | 53,3984 | 0,0696 |
| **PCA** | 0,4636 | 0,6019 | 0,8711 | 13,4026 | 52,9873 | 0,0030 |
| **SWTDCT** | 0,3760 | 0,3511 | 0,7897 | 24,4114 | 53,9247 | 0,8698 |
| **SWT** | 0,5724 | 0,6522 | 0,9038 | 19,6422 | 53,8438 | 0,0398 |
| **ABC** | 0,7170 | 0,8764 | 0,9815 | 24,7407 | 60,4575 | 2,2242 |
| **JS** | 0,7188 | 0,8786 | 0,9816 | 24,7687 | 60,4612 | 1,4493 |

Numerical fusion results of Figure 2 (c) and (d) source image are given in Table 2. As seen from Table 2, it has been experimentally analyzed that JSA is the best in terms of all quality metrics. In addition, it is analyzed that the second best method is the ABC method and the third method is the DCHWT method in terms of all metrics. In comparison of the CPU time consumptions of methods to accomplish the image fusion, it is seen in Table 2 that the fastest is PCA method, the second fastest method is DWTPCA method, and the third fastest method is the SWT method.

**Table 3**: *Numerical results of the quality metrics of compared fusion methods by using source images (e) and (f) in Figure 2.*

| Fused image 3 | Qp_ABF | QSCD | Qy | QSF | Qstd | CPU Time |
|---|---|---|---|---|---|---|
| **DWTPCA** | 0,7062 | 0,2144 | 0,9711 | 16,9740 | 58,0915 | 0,0054 |
| **DCHWT** | 0,7245 | 0,3255 | 0,9681 | 19,6180 | 58,5238 | 0,5989 |
| **APCA** | 0,7219 | 0,2126 | 0,9599 | 13,8119 | 57,6983 | 0,0712 |
| **PCA** | 0,7217 | 0,2151 | 0,9597 | 13,8137 | 57,7072 | 0,0016 |
| **SWTDCT** | 0,6299 | 0,1747 | 0,9468 | 19,4881 | 58,1494 | 0,8711 |
| **SWT** | 0,7370 | 0,2881 | 0,9685 | 18,7292 | 58,2420 | 0,0254 |
| **ABC** | 0,7496 | 0,3920 | 0,9675 | 20,8022 | 59,0853 | 2,6699 |
| **JS** | 0,7495 | 0,3923 | 0,9674 | 20,8127 | 59,0880 | 3,3527 |

In Table 3, fusion results of Figure 2 (d) and (e) source images by using DWTPCA, DCHWT, APCA, PCA, SWTDWT and SWT, ABC and JSA methods are analyzed with various quality metrics. As can be seen from Table 3, JSA is the best method in terms of QSCD, QSF, Qstd quality metrics, ABC method is best for Qp_ABF quality metric and DWTPCA method is best in Qy metric. It is shown that the second best performing method is ABC in terms of QSCD, Qy, QSF and Qstd metrics and JSA according to Qp_ABF metric with. The third best performing method is the SWT method according to Qp_ABF metric, the DCHWT method in terms of QSCD, QSF and Qstd metrics and the JSA method according to Qy metric. As can be seen in Table 4; the numerical fusion results of Figure 2 (g) and (h) source images shows that the JSA method is the best among all methods in terms of Qp_ABF, QSCD and Qstd quality metrics and the second best in terms of Qy and QSF metrics. Table 4 shows that ABC performs best in terms of Qy and QSFmetrics, and the second best in terms of Qp_ABF, QSCD and Qstd. It is understood that the method with the third best performance is the DCHWT method in all metrics.

## 4.2. Visual Results

Quantitative evaluations alone are not sufficient in the comparison of multi-focus image methods, and the necessity of subjective evaluation on visual results in addition to quantitative evaluation emerges. In this section, the visual results obtained in the experiments are given in Figure 3-6. Figure 3 shows the visual fusion results of source images Figure 2 (a) and (b), Figure 4 shows the visual fusion results of source images Figure 2 (c) and (d), Figure 5 shows the visual fusion results of source images Figure 2 (e) and (f) and Figure 6 shows the visual fusion results of source images Figure 2 (g) and (h).

**Table 4:** *Numerical results of the quality metrics of compared fusion methods by using source images (g) and (h) in Figure 2.*

| Fused image 4 | Qp_ABF | QSCD | Qy | QSF | Qstd | CPU Time |
|---|---|---|---|---|---|---|
| **DWTPCA** | 0,6093 | 0,3622 | 0,9382 | 16,3340 | 56,5882 | 0,0053 |
| **DCHWT** | 0,7016 | 0,5320 | 0,9644 | 24,8752 | 58,7827 | 0,5886 |
| **APCA** | 0,5894 | 0,3647 | 0,9301 | 15,0507 | 56,6104 | 0,0714 |
| **PCA** | 0,5885 | 0,3631 | 0,9301 | 15,0290 | 56,6035 | 0,0012 |
| **SWTDCT** | 0,4761 | 0,3125 | 0,9025 | 24,2544 | 57,8108 | 0,8777 |
| **SWT** | 0,6743 | 0,4519 | 0,9550 | 21,8141 | 57,4821 | 0,0289 |
| **ABC** | 0,7437 | 0,5783 | 0,9737 | 26,3156 | 59,7224 | 3,2552 |
| **JSA** | 0,7438 | 0,5793 | 0,9736 | 26,3153 | 59,7259 | 4,1596 |

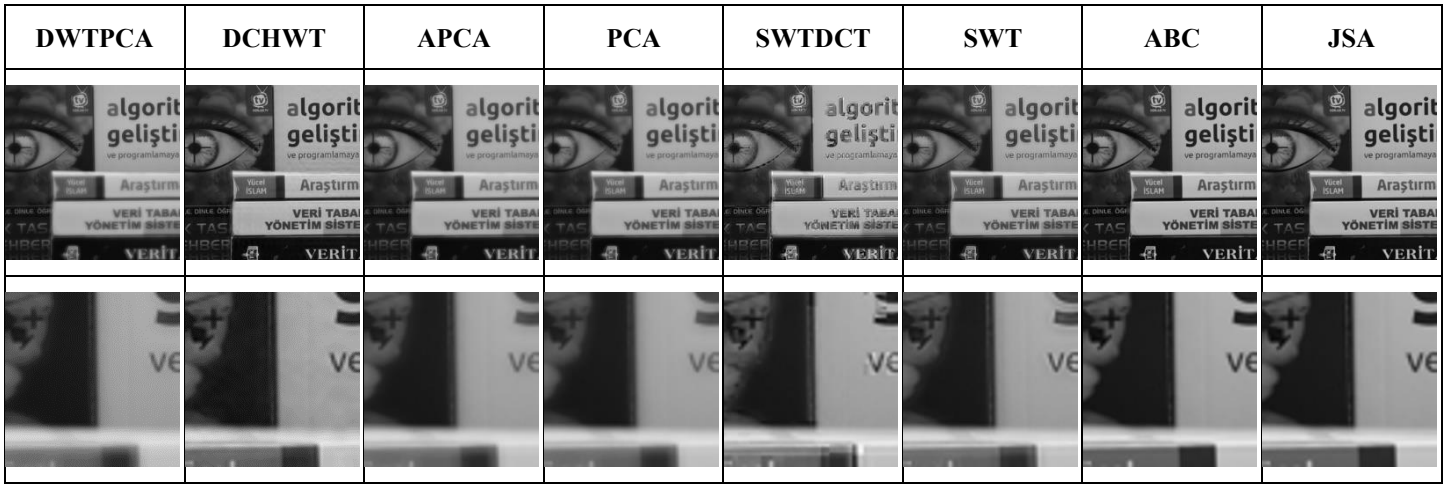


***Figure 3**: Visual fusion result of Figure 2 (a) and (b) and magnifications of a particular region in the resulting images.*

As shown in Figure 5 and Figure 6, it is seen that the fused images obtained by using JSA and ABC methods have a minimum level of blurness, however there are errors in the transition regions in the images obtained of other methods.

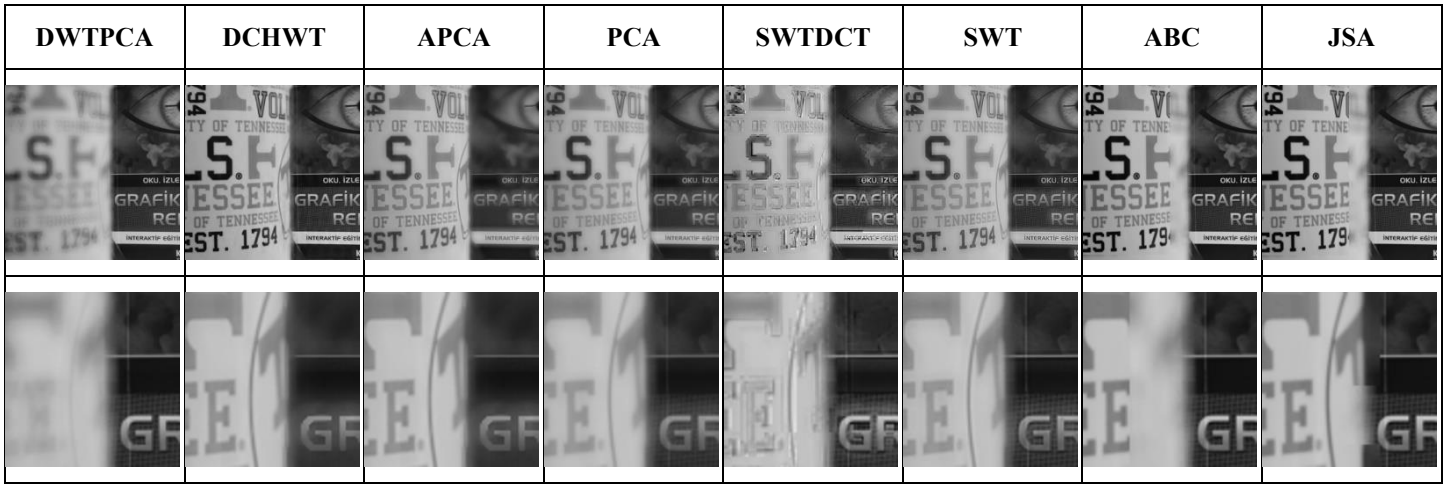


***Figure 4:*** *Visual fusion result of Figure 2 (c) and (d) and magnifications of a particular region in the resulting images*

When the fused images in Figure 3 and Figure 4 are examined, it is seen that the fusion images obtained by the JSA method in a near-perfect manner in terms of sharpness. On the other hand, while ABC and DCHWT methods exhibited successful merging performance, it is noteworthy that there is blur in the combined images obtained from SWTDCT, DWTPCA and SWT methods.

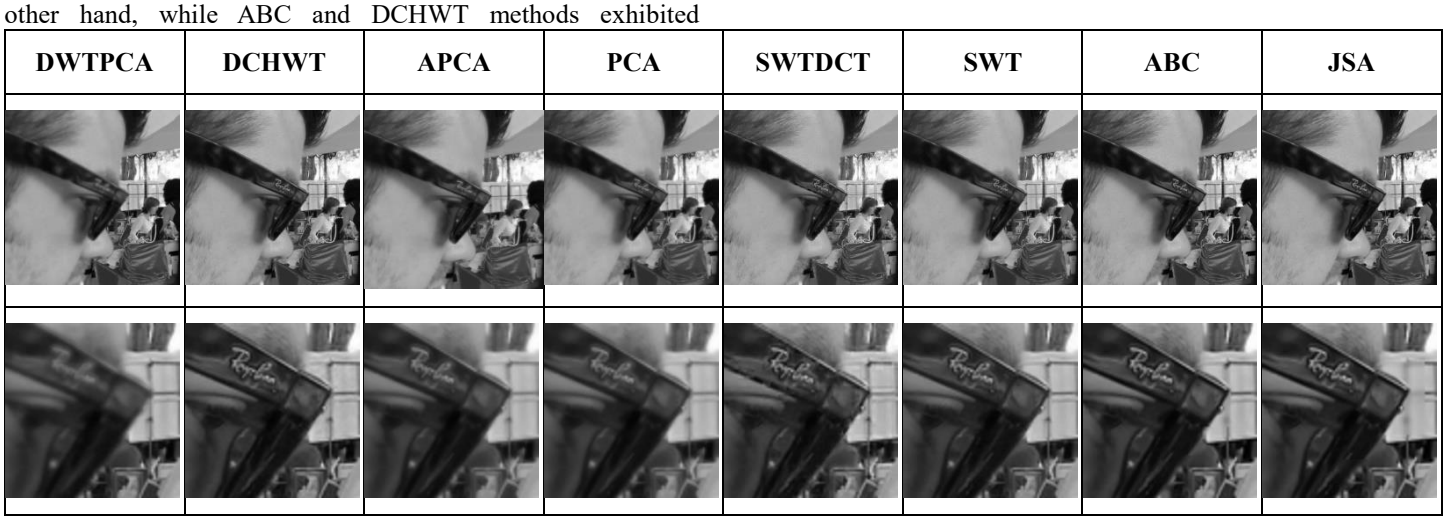


***Figure 5:*** *Visual fusion result of Figure 2 (e) and (f) and magnifications of a particular region in the resulting images*

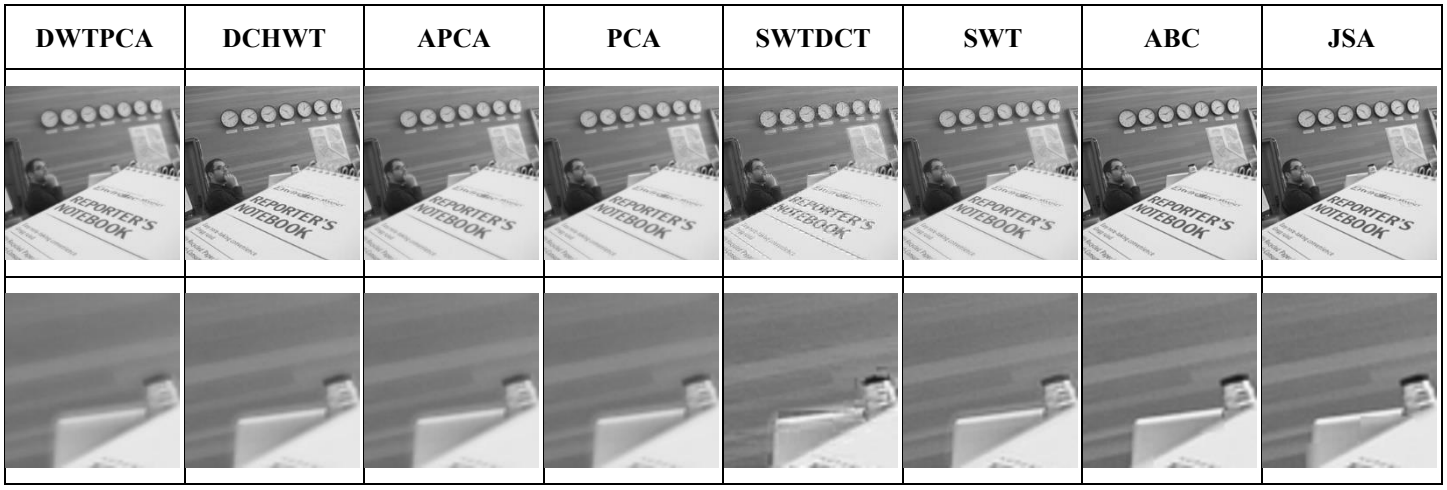


***Figure 6:*** *Visual fusion result of Figure 2 (g) and (h) and magnifications of a particular region in the resulting images*

## 5. Conclusions

In this study, an efficient and robust multifocus image fusion method is presented by selecting image blocks that are sharper than source images with JSA. A comparison is realized between the proposed method and the ABC algorithm, which is one of the metaheuristic methods, as well as DWTPCA, DCHWT, APCA, PCA, SWTDWT and SWT methods. Performance comparison of the methods are conducted using objective quality metrics such as Qp_ABF, QSCD, Qy, QSF and Qstd. From the experimental results, it is understood that the JSA method outperforms other methods visually and quantitatively. Also, the JSA method can converge to the optimal solution faster than the ABC method.

## 6. Acknowledgements

This research is financially supported by Kayseri University Scientific Research Projects Unit under the grant number FYL-2022-1051.

## References

Agrawal, S., Swain, S., & Dora, L. (2013, April). BFO-ICA based multi focus image fusion. In 2013 IEEE Symposium on Swarm Intelligence (SIS) (pp. 194-199). IEEE.

Aslantas, V., & Bendes, E. (2015). A new image quality metric for image fusion: The sum of the correlations of differences. AEU-International Journal Of Electronics And Communications, 69(12), 1890-1896.

Aslantas, V., & Kurban, R. (2010). Fusion of multi-focus images using differential evolution algorithm. Expert Systems with Applications, 37(12), 8861-8870.

Aslantas, V., & Toprak, A. N. (2014). A pixel based multi-focus image fusion method. Optics Communications, 332, 350-358.

Bai, X., Liu, M., Chen, Z., Wang, P., & Zhang, Y. (2016). Multi-focus image fusion through gradient-based decision map construction and mathematical morphology. IEEE Access, 4, 4749-4760.

Banharnsakun, A. (2019). Multi-focus image fusion using best-so-far abc strategies. Neural Computing and Applications, 31(7), 2025-2040.

Bastian, T., Lilley, M. K., Beggs, S. E., Hays, G. C., & Doyle, T. K. (2014). Ecosystem relevance of variable jellyfish biomass in the Irish Sea between years, regions and water types. Estuarine, Coastal and Shelf Science, 149, 302-312.

Brotz, L., Cheung, W. W., Kleisner, K., Pakhomov, E., & Pauly, D. (2012). Increasing jellyfish populations: trends in large marine ecosystems. In Jellyfish blooms IV (pp. 3-20). Springer, Dordrecht.

Cao, L., Jin, L., Tao, H., Li, G., Zhuang, Z., & Zhang, Y. (2014). Multi-focus image fusion based on spatial frequency in discrete cosine transform domain. IEEE Signal Processing Letters, 22(2), 220-224.

Chou, J. S., & Truong, D. N. (2021). A novel metaheuristic optimizer inspired by behavior of jellyfish in ocean. Applied Mathematics and Computation, 389, 125535.

Dong, Z., Liu, D., & Keesing, J. K. (2010). Jellyfish blooms in China: dominant species, causes and consequences. Marine Pollution Bulletin, 60(7), 954-963.

Dorigo, M., Birattari, M., & Stutzle, T. (2006). Ant colony optimization. IEEE Computational Intelligence Magazine, 1(4), 28-39.

Eskicioglu, A. M., & Fisher, P. S. (1995). Image quality measures and their performance. IEEE Transactions on Communications, 43(12), 2959-2965.

Fossette, S., Gleiss, A. C., Chalumeau, J., Bastian, T., Armstrong, C. D., Vandenabeele, S., & Hays, G. C. (2015). Current-oriented swimming by jellyfish and its role in bloom maintenance. Current Biology, 25(3), 342-347.

Fossette, S., Putman, N. F., Lohmann, K. J., Marsh, R., & Hays, G. C. (2012). A biologist's guide to assessing ocean currents: a review. Marine Ecology Progress Series, 457, 285-301.

Garg, R., Gupta, P., & Kaur, H. (2014, March). Survey on multi-focus image fusion algorithms. In 2014 Recent Advances in Engineering and Computational Sciences (RAECS) (pp. 1-5). IEEE.

Ardeshir Goshtasby, A., & Nikolov, S. (2007). Guest editorial: Image fusion: Advances in the State of the Art. Information Fusion, 8(2), 114-118.

Irshad, H., Kamran, M., Siddiqui, A. B., & Hussain, A. (2009, December). Image fusion using computational intelligence: A survey. In 2009 Second International Conference on Environmental and Computer Science (pp. 128-132). IEEE.

Li, S., Hong, R., & Wu, X. (2008, July). A novel similarity based quality metric for image fusion. In 2008 International Conference on Audio, Language and Image Processing (pp. 167-172). IEEE.

Li, S., Kwok, J. T., & Wang, Y. (2001). Combination of images with diverse focuses using the spatial frequency. Information Fusion, 2(3), 169-176.

Liu, Y., Wang, L., Cheng, J., Li, C., & Chen, X. (2020). Multi-focus image fusion: A survey of the state of the art. Information Fusion, 64, 71-91.

Mariottini, G. L., & Pane, L. (2010). Mediterranean jellyfish venoms: A Review On Scyphomedusae. Marine Drugs, 8(4), 1122-1152.

Meher, B., Agrawal, S., Panda, R., & Abraham, A. (2019). A survey on region based image fusion methods. Information Fusion, 48, 119-132.

Nejati, M., Samavi, S., Karimi, N., Soroushmehr, S. R., Shirani, S., Roosta, I., & Najarian, K. (2017). Surface area-based focus criterion for multi-focus image fusion. Information Fusion, 36, 284-295.

Nejati, M., Samavi, S., & Shirani, S. (2015). Multi-focus image fusion using dictionary-based sparse representation. Information Fusion, 25, 72-84.

Phamila, Y. A. V., & Amutha, R. (2014). Discrete Cosine Transform based fusion of multi-focus images for visual sensor networks. Signal Processing, 95, 161-170.

Vijayarajan, R., & Muttan, S. (2015). Discrete wavelet transform based principal component averaging fusion for medical images. AEU-International Journal of Electronics and Communications, 69(6), 896-902.

Wang, Z., Ziou, D., Armenakis, C., Li, D., & Li, Q. (2005). A comparative analysis of image fusion methods. IEEE Transactions On Geoscience And Remote Sensing, 43(6), 1391-1402.

Xu, J., & Zhang, J. (2014, July). Exploration-exploitation tradeoffs in metaheuristics: Survey and analysis. In Proceedings of the 33rd Chinese control conference (pp. 8633-8638). IEEE.

Xydeas, C. S., & Petrovic, V. (2000). Objective image fusion performance measure. Electronics Letters, 36(4), 308-309.

Zavodnik, D. (1987). Spatial aggregations of the swarming jellyfish Pelagia noctiluca (Scyphozoa). Marine Biology, 94(2), 265-269.

Zhang, Y., Liu, Y., Sun, P., Yan, H., Zhao, X., & Zhang, L. (2020). IFCNN: A general image fusion framework based on convolutional neural network. Information Fusion, 54, 99-118.